3D PRINTED ORTHOSIS EVALUATION

By

Jay Segel - DPM

Deepthi Priyanka Mallela - MBBS and MPH

Sally Crawford - MS

PRIMARY OBJECTIVE

To evaluate the effect of a 3D printed functional orthosis on the human foot, in standing balance and dynamic gait.

EXECUTIVE SUMMARY

The growing want for 3D printed products and innovation pairs nicely with the increasing demand for precision foot orthosis, and so, there is a resultant need for objective testing and validation. To initiate a framework for developing this better understanding, measuring the effects of 3D printed orthosis on human stance and gait with as few interacting variables as possible is needed. Isolating the influence of patient-specific 3D printed orthosis without the contribution of footwear allows for a more accurate assessment of efficacy and cleaner conclusions when comparing metrics over three data sets, barefoot baseline, accepted norms and the orthosis clad foot. This single-center observational study on a sample cohort of 30 participants was designed to qualify and quantify the effect of a 3D printed functional orthosis, when secured directly against the foot and acting upon walking surface.

For this study, the protocols for testing and analysis were uniquely designed to compare a participant's baseline barefoot reading to the wearing of the 3D printed device. Efficacy was judged by biomechanical principles and data tending towards, or away from published norms when such norms exist. These standardized protocols involved measuring all the spatial, temporal, and zonal results from walking in barefoot and with the orthosis. The 3D printed orthosis was affixed to each of the participants' plantar surfaces (left and right foot) with a carefully chosen top dressing sleeve. The recordings for each participant were >15 strides in length and for standing balance included >10 seconds in length. The data collection was performed using a standardized, calibrated pressure instrumented treadmill and research-grade integrated software and video capture, making temporal and spatial parameter calculations possible. Through these disciplined practices and approaches, more than 200 useful biomechanical markers that characterize the effects of the 3D printed orthosis were gathered and analyzed.

From the analysis of gathered data, both barefoot and orthosis clad, compared to established norms, we can state that there are several statistically significant findings in dynamic function. Of note was an improved purchase with the ground, pronation control, more optimally distributed weight, and gait stability as well as variability. Statically, standing balance results were trending in that all participants had more optimal resulting positional and pressure re-distribution with the wearing of the device compared to the baseline recordings. The conclusions from this N=30 efficacy study qualitatively and quantitatively explain the effects of the functional 3D printed orthosis on gait and demonstrate statistically significant positive trends in both spatial and temporal gait parameters when compared to the baseline normative data.

TABLE OF CONTENTS

INTRODUCTION

3D printing of medical devices is an evolving technology with an emphasis on rapid development, fabrication, and methodology. This growing technology, in association with its use in 3D printed orthosis is requiring more objective understanding. To develop a framework for this improved understanding, measuring the influences of 3D printed orthosis on human gait is needed. Quantifying the influence of patient-specific 3D printed orthosis in comparison to normative and barefoot data that determine the true benefits of the device on an individual's gait and balance without the influence of footwear is a groundbreaking endeavor.

When examining an individual's gait and balance, objective measures are often lacking. Outcomes or product efficacy results are commonly based on injury rates or patient-reported outcomes, which are subjective. To better understand such outcomes more objectively, gait and balance variables, including but not limited to improved symmetry between sides, symmetry indices and variability in gait and temporal and spatial variables researched. [1] [2] [3]

It is commonly found in performance-oriented studies that testing gait patterns provides a standardized method for assessing and monitoring biomechanical asymmetries.[4] [5] [6] [7] Asymmetry in walking gait has been shown, through both randomized controlled studies and meta-analyses of such studies, to be detrimental to performance.[8] [9] In an optimal world where gait abnormalities, fatigue and injury are absent, gait parameters should trend towards longer steps and stride length, increased cadence, prolonged stance and double support phase, smaller more balanced base of support and a longer single support phase).[10] [11] Standing balance parameters should trend towards equal loading through left and right sides. [12] With improvements in such variables coupled with more optimal side to side symmetries, injury risk is reduced, and gait economy is enhanced. [13]

Aside from the more global quantifications of side-to-side symmetry and function, gait stability, and variability, frequently published works focus on gait temporal (Image 1b) and spatial metrics during dynamic gait. Given these domains of variables are not usually published together, but examined in isolation, there is a gap in understanding how the complete gait and balance variables impact one another. To narrow this gap and provide more insight to the combined domains of biomechanical metrics, learning of Computerized Gait Analysis, or CAGA, was introduced. [14] With such CAGA tools, understanding of all-encompassing gait metrics and their additional impact in understanding objectively optimized clinical outcomes can be achieved.

INTRODUCTION TO COMPUTER-AIDED GAIT ANALYSIS (CAGA) REPORTING

Computerized systems that provide these metrics are varied, so the importance of selecting research grade solutions offering easy and accurate repeatability is important. The discipline of traditional pressure and gait biomechanics is driven by two sets of parameters. Spatial data deals with items like foot positioning, event length and width, whereas temporal parameters are based on the premise that every gait event is happening at specific times and in a specified order (Image 1a).

Typically, in prior research studies of gait, reporting includes only temporal or spatial parameters and not both. However, there are some measurement solutions that provide a combination of both, as well as center of pressure-focused quantifications and data visualizations (Noraxon U.S.A., Inc, Zebris Medical GmbH, Germany).

A compiled gait report should include four main sections. The first involves the complete spatial and temporal parameters, with timing and left to right symmetries for easy analysis and comparison. The second provides the analysis of the center of pressure (COP) data for each step, left and right stabilities, and an illustration of the total body COP. The third part shows a force loading summary of every step normalized to one full gait cycle, as well as an averaging of the maximum pressure plots with overlaid gait lines. The fourth section is a zonal analysis that identifies above parameters but within only certain zones of the foot (Image 1b). Having all parts of the report rapidly calculated by such research-grade software provides a comprehensive summary of a walking test of any length or speed.

The center of pressure (COP) gait line report is a visual expression of stance phase, represented by the aggregate of pressure and visualized as a set of coordinate points plotted with respect to time and at a specific sample rate of 300ms. The initial coordinate point characterizes initial contact point, usually at the lateral heel, until the termination of the stance phase of gait, which ideally is toe-off. The COP progression explains the heel-to-toe directional movement including varying amounts of pronation. Appropriate pronation in loading is both wanted and needed at foot contact, but prolonged pronation can be detrimental.
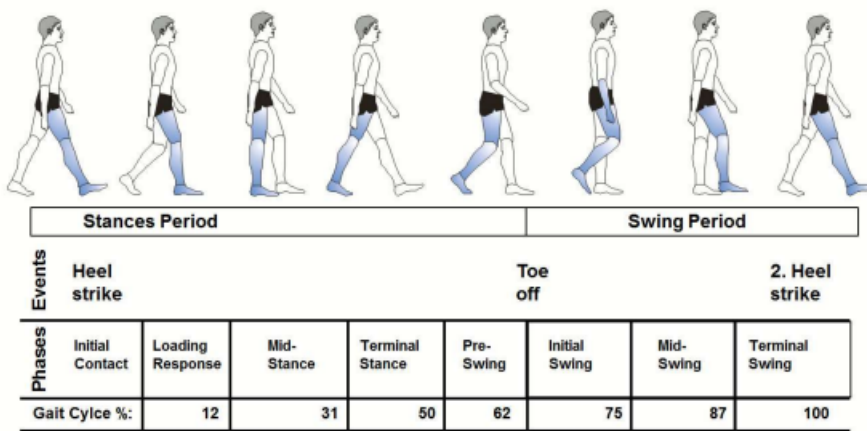

Image 1a: Gait phase definitions included in results
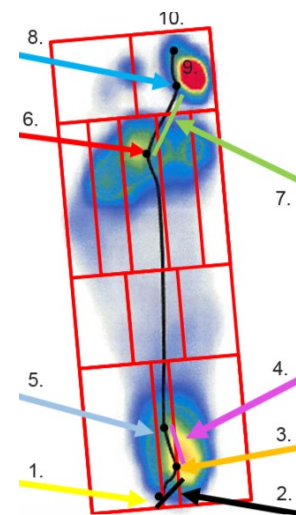
Image 1b: Pressure zones with COP progress and morphological mapping points (Additional details Appendix B).

Ground reaction force (GRF) graphs compiled from every step normalized to one full gait cycle, starting at 0% and ending at the end of stance phase, around 60-63% of a full gait cycle (Image 2). GRF data is derived from formulae of basic Newtonian laws of physics; you hit the ground, the ground hits you back in an equal and opposite manner[15]. Given that we have a three-dimensional foot of limited mass colliding with a relatively two-dimensional support surface of relatively unlimited mass, we can gather data based on the foot and ankle response to this repetitive collision. We can compare GRF graphs of barefoot walking to orthosis intervention and quantify differences in patterns and speed of loading at all points in the stance phase of gait.
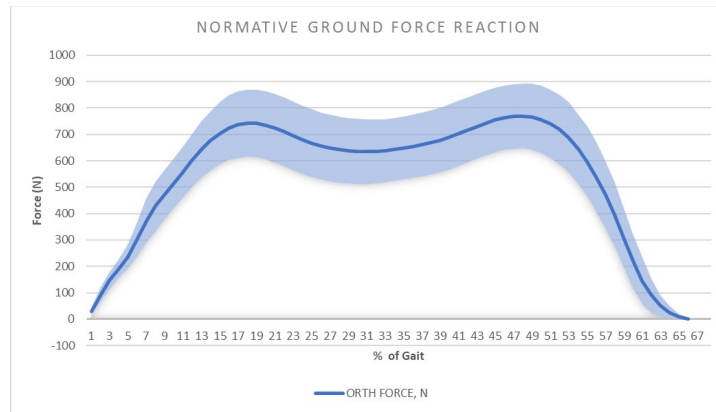
Image 2: Ground reaction force curve sample of loading and off-loading through stance phase.

READING REPORT DATA

When analyzing such comprehensive data during gait, coordinating the temporal, or timing, aspects to the spatial location of the COP at that time is imperative. COP data is visualized as a comprehensive expression of gait through stance phase. COP gait line data begins with the initial impact point (IIP), normally at the heel, and runs until the end terminal double stance, which is typically at toe-off. By comparing two COP gait line visualizations, without and with orthosis intervention, we can see changes in the pressure speed of progression, highlighted by color changes and density of sample rate-based measurements, and changes to the COP line morphology. Understanding the speed of COP progressions allow understanding of locations were motions slow or "bog down". When motion slows in the COP it is representative of the body continuing to move over a foot that is no longer moving with it, i.e. the forces are building and can be damaging because of this delay in progression. Understanding the morphological changes in COP gait line helps identify factors in dynamic gait such as pronation control or adaptations to shock and loading and allows quantified understanding of orthosis effects. COP morphology, learned through CAGA, aids in evaluating and drawing conclusions about the effects of orthosis and their function with the 3D dynamic surface of our feet.

With these tools, gait reporting capabilities allow understanding of the described and validated metrics and help providers, researchers and those specializing in the biomechanics of foot orthosis to approach care and planning in a more objective and evidence-based manner.

CLINICAL PROTOCOL

We use a single-center observational study to evaluate the effects of a 3D printed custom orthosis in October 2021. Steps included screening, selection, scanning of the feet, prescription writing, fitting of orthosis into shoes, and testing. All steps were done by the same Podiatrist and at the same location to minimize variation, apart from orthosis fabrication which was done by Arize/HP.

PRESELECTION CONSIDERATIONS/INCLUSION AND EXCLUSION CRITERIA

We recruited a cohort of 30 patients and 4 alternates of varying age, height, weight, activity levels, and foot/gait issues who stated they could walk comfortably at 2.5 mph and had some familiarity with orthosis. Participants

were not excluded based on foot type, but rather, exclusion criteria included those in poor general health, anyone who had a recent fracture or joint replacements, anyone with open wounds on the lower extremity, anyone with severe peripheral neuropathy, diminished mental capacity, systemic neurological conditions such as Parkinson's, significant gait maladies (i.e. drop foot), amputation of the lower limb, minors, as well as practical issues like availability and schedule accommodation.

After the prescreening process, selected participants were fully informed as to the study being undertaken, the scope, their rights and responsibilities and all questions were answered to assure subject clarity. Participants consented both verbally and using a scripted consenting process (See Appendix: Participant Consent and Protocol Overview). All participants had no prior adaptation to 3D printed orthosis, and, assented to be contacted in consideration for further or evolving study participation. Adaptation can be defined as a period of no more than 10% of daily step volume up or up to a maximum of 10 minutes per day in 3D printed orthosis.[16]

Visit 1: Evaluation including local exam, scheduled scan, explained below, and with the consented participant - Participants were greeted by a principal investigator and Office Administrator and cleared following Covid entry and safety protocols at the Segel Podiatry practice in Martha's Vineyard. Demographics were reconfirmed and entered into the electronic health record. All participants were assigned an "HP number" in anticipation of the removal of identifying personal health information.

3D SCAN PROCESS AND IMAGING

Subject 3D foot scans were performed bilaterally after sole practitioner positioning to accomplish uniformity of technique and placement. A semi-weight bearing image was obtained with the medial longitudinal arch centered by the white hash mark on the scanner, while the subject was seated upright and comfortable with knee situated at 90 degrees from the foot. After demographic data entry, image capture was achieved by use of the HP 3D Laser Foot Scanner and viewed in the HP proprietary user interface created to receive, view, and interact with these images. These 3D digital images of the foot are used as a modern casting technique from which the orthosis will be generated. This software is outfitted with a complete orthosis ordering system for comprehensive prescription writing.

The Arize orthoses are 3D printed using HP Multi Jet Fusion (MJF) technology, customized to match the subject's scan and to follow the prescriber's design requirements. Once the shells are printed, they are then manually covered with the prescriber's preferred top cover option. All ordered orthosis for this study were printed in the same location, using the same printer and we quality checked by the same person.

In between visits, co-primary investigator completed orthosis prescription writing, adding only the standardized attributes below (Image 3):

- HP/Arize functional device style,
- 1 mm heel lift bilateral
- 12 mm heel cup depth
- Wide/Athletic cut heel cup width
- Bambalon top cover with 1/8 inch poron padding to sulcus

Image 3: Sample 3D Printed Orthosis Device

Following orthosis prescription submission, the devices were received, examined for defects, and logged in.

Visit 2: Scheduling was set to 30 min increments per participant.

Participants were greeted by Head Study and Office Administrator and cleared following Covid entry and safety protocols at the Segel Podiatry practice in Martha's Vineyard. On this second pre-scheduled visit participants were additionally introduced to Head Technician and explained the protocol of 12 tests they would be completing.

Our testing protocol always began with a barefoot standing data capture, with hip width heel placement and natural foot placement angle recorded for 10+ seconds in length on the pressure platform, in a flat position. Following the barefoot baseline, the participants were captured for 10+ more seconds with the orthosis in place under their feet, maintaining the same foot placement coordinates on the platform.

Following the static standing balance recordings, Visco-GEL® Sleeves were worn with dorsally placed gel and participants were instructed to walk on the treadmill for 30 seconds at an initial speed of 1.5mph and then another 30 seconds at 2.5mph while data was collected at both speeds. Wearing the gel during baseline walking recordings eliminated influences from the Visco-GEL® Sleeves. Following the Barefoot walking with the Visco-GEL® Sleeve, prescribed precision 3D printed orthosis were secured by practitioner following protocol using Nexcare flexible clear Transpore tape in five locations across the orthosis surface and wrapping around to the top of the foot, and at a distal and proximal position of foot (Image 4). Over the orthosis, the same Visco-GEL® Sleeves were worn both left and right side (Image 5a). With sleeve and orthosis in place, Participants were instructed to walk on the treadmill for 30 seconds at an initial speed of 1.5mph and then another 30 seconds at 2.5mph while data was collected at both speeds (Image 5b).

Image 4: 3D printed orthosis device fixation process

Image 5a: Fixation sleeve   **Image 5b:** Walking with fixation sleeve

TECHNICAL SPECIFICATIONS

Testing at visit two was completed on a medical grade treadmill. Gait spatial, temporal and center of pressure parameters were obtained using the research grade Zebris FDM-T Treadmill (Zebris1 Medical GmbH, Germany) fitted with an under-belt platform consisting of 10,240 force sensors, each approximately 1 cm × 1 cm. During walking and static standing reactive-normal force in directions x, y and z are recorded by the sensors at a sampling rate of 120 Hz. Due to the high density of the sensors, the foot is mapped at a high resolution to facilitate even subtle changes in force distribution. Timing can also be monitored and standardized in a fashion allowing adequate repeat testing[17]. Dedicated Noraxon MyoResearch Software 3.18.08 running static and dynamic hardware configurations in expert 10 zone mode, integrates the force signals and provides 2D/3D graphic representation. From the parameters analyzed from the 100% gait normalized measurement there were additional parameters calculated characterizing the interlimb symmetry[18].

Additionally, synchronized to the pressure outfitted treadmill, three slow-motion high-definition cameras in synchronization with FDM-T/MR3 Ninox cameras were streaming, and one slow-motion high-definition camera in sync with FDM-T/MR3 Logitech C 920.

Given gait raw force data was available, gait cycle normalized force curves were possible to construct, representing an averaged summary of every step. Given the analyzed metrics from the average for each step, left and right calculations of all parameters were possible to compare. Symmetry refers to the exact replication or similarity of one limb's movement by the contralateral side, with asymmetry referring to any deviation from symmetry.[19] [20]

STATISTICAL METHODS

The baseline characteristics of participants in the HP study evaluating the 3D printed orthosis device were explored. The descriptive analyses were performed and the demographic characteristics along with gait parameters at baseline were reported in Table. 1. The categorical variables were reported as n (%) and continuous variables in appropriate variable measurement units.

Second, all the computer assisted gait parameters were compared between barefoot baseline and orthosis in both static and dynamic conditions. Paired sample *t-tests* were used to compare the means of gait parameters

between the orthosis and baseline. Mean differences in gait parameters and p-values were computed for each gait parameter variable to assess the statistically significant gait parameters. The univariate analyses were performed for gait parameters recorded in both dynamic (Table 2) and static conditions (Table 3). All the variables that yielded a p-value of <0.05 were noted as statistically significant.

Third, multivariable linear regression analyses were performed to assess the association of the gait parameters with the 3D printed orthosis in both static and dynamic conditions. All the gait parameters that had a p-value <0.2 were selected from the analyses (Table 2) and were included in the final multivariable models. A backward stepwise linear regression analysis with pr (0.2) and pe (0.1) criteria was used to assess the association of significant gait parameters with the 3D printed orthosis device after controlling for patient baseline characteristics and other gait parameters.

All model fits were assessed using R-squared and adjusted R-squared. All statistical analyses were performed using Stata version 16.1 (StataCorp. 2019. Stata Statistical Software: Release 16. College Station, TX: StataCorp LLC.)

RESULTS

The descriptive analysis of participants along with gait parameters at baseline are reported in Table 1.

**Table 1:** Participant Characteristics and Baseline Gait Parameters

Variables	Number of participants, n (%)
Demographics	
Age	
<65 (Average <65 = 50.5yr)	18 (56.3%)
≥65 (Average >65 = 69.8yr)	14 (43.8%)
Gender	
Male (Average 57.2yr)	15 (46.9%)
Female (Average 60.4yr)	17 (53.1%)
Body mass index	
Underweight (<18.5 kg/m^2)	2 (6.3%)
Normal (18.5 – 24.9 kg/m^2)	13 (40.6%)
Overweight (25-29.9 kg/m^2)	11 (34.4%)
Obese (≥30 kg/m^2)	6 (18.8%)
Selection of Pressure Mapping Gait Parameters	**Mean ± SD (IQR)**
Length of gait line (right), mm	253.9 ±19.5 (185.7 – 283.7)
Length of gait line (left), mm	256.2 ± 16.4 (227.1 – 286.2)
Anterior-posterior position, mm	143.8± 11.9 (122.3 – 181.8)
Average lateral symmetry, mm	2.2±6.2 (-8.2 – 25.7)
Stance phase (left), %	65.2±2.3 (61.4 – 70.5)
Stance phase (right), %	65.0±2.4 (59.7 – 71.5)
Step width, cm	8.9±3.5 (3.1 – 17.0)
Ten zones Peak force RT Heel Center [N]	94.9 ± 23.6 (74.5 – 112.3)
Ten zones Start RT Heel Lateral	0.02 ± 0.10 (0.0 – 0.5)
Ten zones Peak force LT Heel Center [N]	95.6 ± 22.7 (78.9 – 111.9)
Ten zones Start LT Heel Lateral	0.03 ± 0.14 (0.0 – 0.5)
Asymmetry Parameters	**Mean ± SD (IQR)**
Asymmetry in gaitline	0.009 ± 0.014 (0.004 – 0.010)
Asymmetry in gaitline variability	0.22 ± 0.21 (0.053 – 0.368)
Asymmetry in single support	0.05 ± 0.07 (0.01 – 0.05)

|	
Asymmetry in single support variability	0.13 ± 0.09 (0.06 – 0.20)
Asymmetry in support Phase	0.007 ± 0.006 (0.003 – 0.009)
Asymmetry in support phase variability	0.13 ± 0.09 (0.05 – 0.20)
Asymmetry in loading response	0.037 ± 0.035 (0.012 – 0.047)
Asymmetry in loading response variability	0.11 ± 0.08 (0.05 – 0.16)
Asymmetry in single support phase	0.012 ± 0.009 (0.005 – 0.015)
Asymmetry in single support phase variability	0.041 ± 0.162 (0.04 – 0.16)
Asymmetry in preswing phase	0.037 ± 0.035 (0.014 – 0.047)
Asymmetry in preswing phase variability	0.108 ± 0.092 (0.04 – 0.16)
Asymmetry in swing phase	0.012 ± 0.009 (0.005 – 0.0157)
Asymmetry in swing phase variability	0.130 ± 0.09 (0.048 – 0.200)
Asymmetry in Foot rotation	1.41 ± 9.65 (0.051 – 0.274)
Asymmetry in foot rotation variability	0.104 ± 0.083 (0.038 – 0.162)
Asymmetry in step length	0.02 ± 0.02 (0.006 – 0.030)
Asymmetry in step length variability	0.113 ± 0.08 (0.04 – 0.15)

For demographics, data were reported as n (%) and for gait parameters, data were reported as mean ± SD (IQR); SD: standard deviation; IQR: interquartile range

DYNAMIC WALKING GAIT RESULTS

Results indicated that this 3D printed orthosis had a significant effect on the foot during dynamic walking. Through stance phase statistically significant improvements in the average length of gait line resulted bilaterally with 3D printed orthosis device compared to barefoot ($p < 0.001$) (Image 6a, 7). Similarly, in stance and swing phase more forward motion of the COP resulted (Image 6b, 8). **A lengthened or prolonged COP contact and stance phase with more forward motion in gait progression tend to coincide with reduced injury rates.**


BF   ORTH
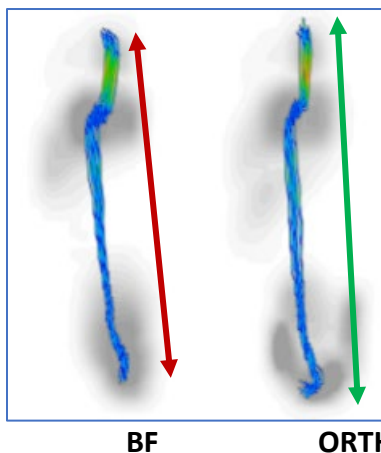
Image 6a: Increased COP path length with orthosis

BF   ORTH
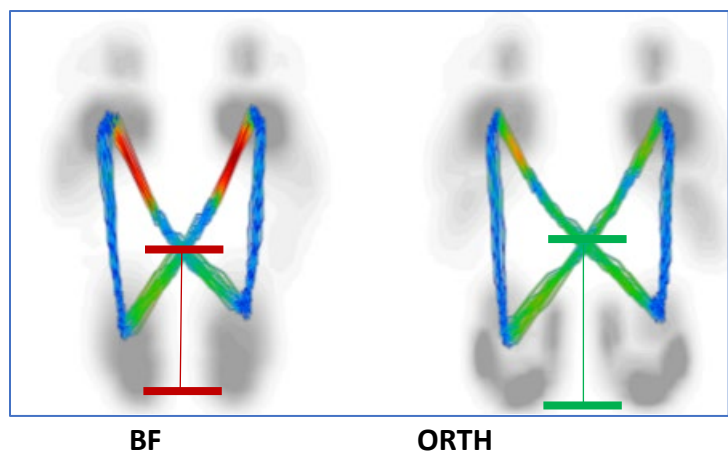
Image 6b: More anterior COP progression
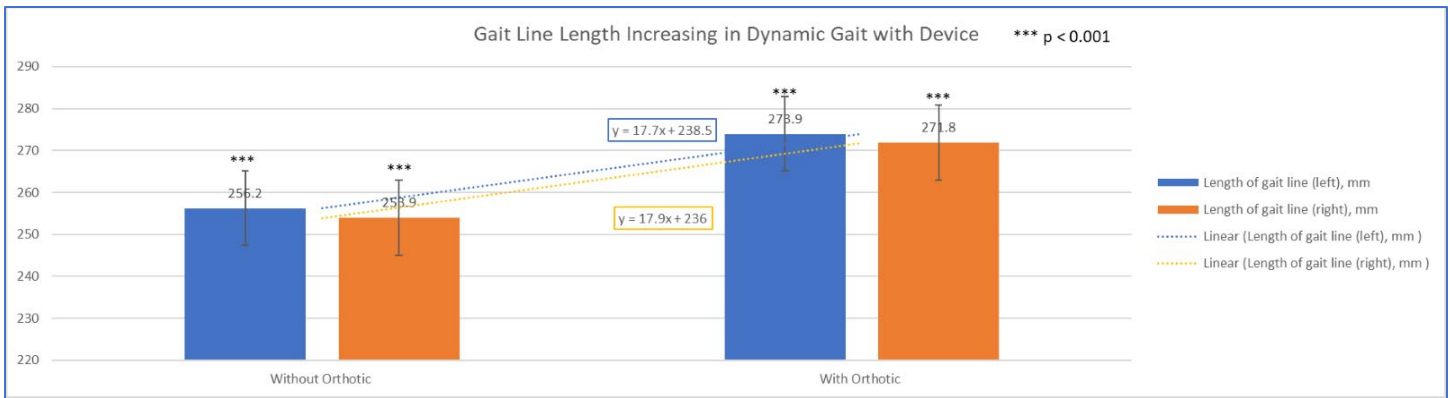
**Image 7:** Gait Line Length Increasing in Dynamic Gait with Device
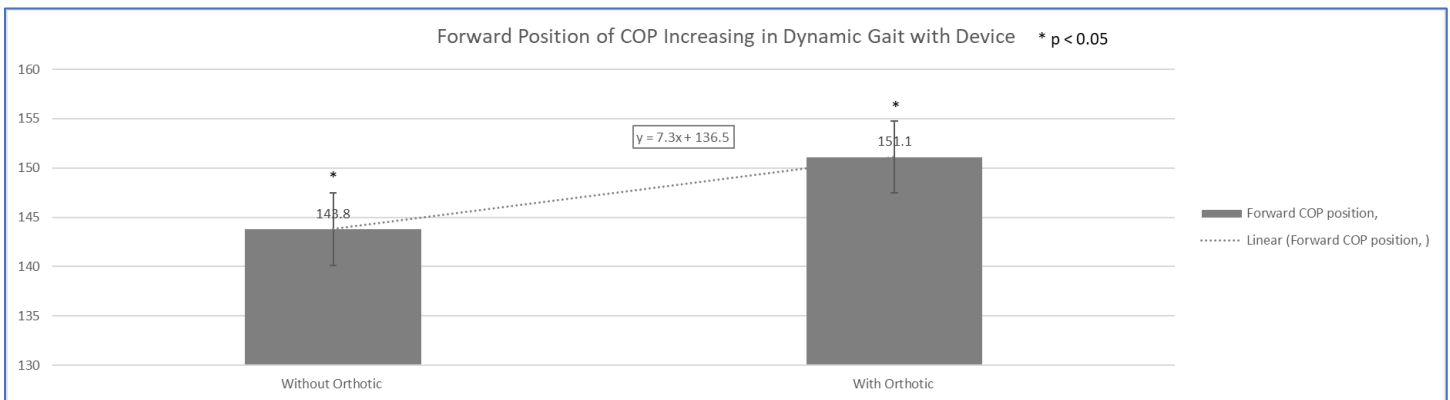
Image 8: Forward/Anterior Positioning of COP in gait with device.

In addition to the anterior, posterior lengthening there were improvements in the medial lateral COP motions with orthosis (Image 9). Lateral motions became more central indicating less variability in base of support and deviations from side to side. Additionally, every participant walked with varying degrees of external or internal rotation during trials. The difference in variability of external rotation between barefoot and orthosis trials showed a decrease in this variable. In the multivariable linear regression analyses of dynamic gait data, where all other parameter interactions and cohort characteristics are considered, the variability in "foot rotation" was decreased by 0.131 degrees (95% CI: -0.224 - -0.038) degrees with orthosis compared to baseline barefoot. The ipsilateral "foot rotation" was also independently associated with ipsilateral step length, variability in step width, and variability in contralateral "foot rotation" (refer Table 3). **Overall improvement in side-to-side shifting and variability in placement proves more optimal stability through gait with orthosis.**
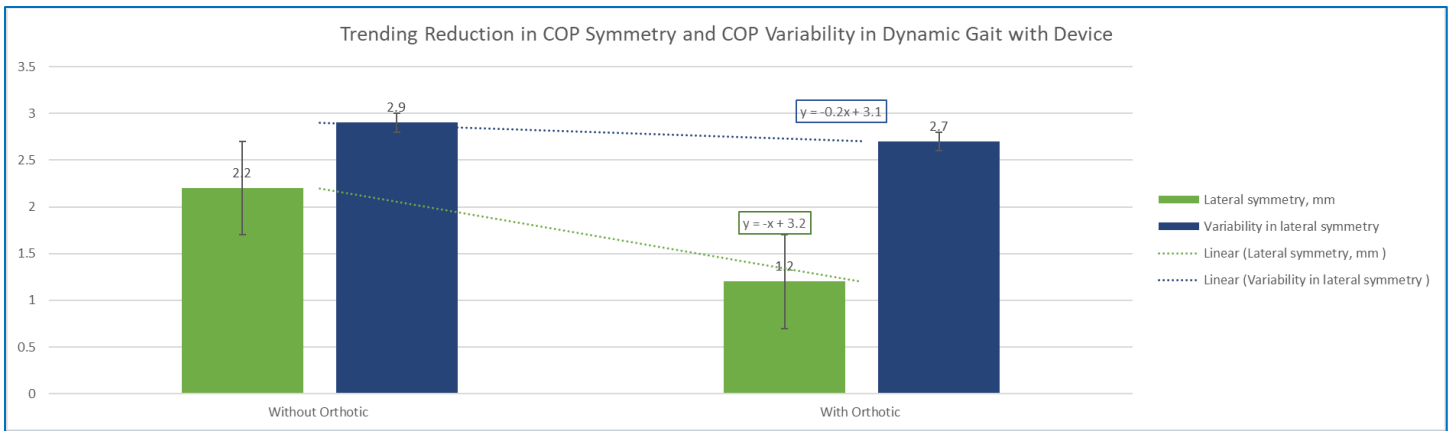
Image 9: Trending improvement in COP symmetry and variability in walking gait with orthosis.

Statistically significant findings of central heel pressure reduction ($p<0.001$) as well as correlations from the linear regressions on the shift forward of the center of pressure during gait with device ($p<0.01$) resulted (Table 2). This is shown graphically for each participant as seen in examples below (Image 10a). Improved pressure redistribution away from the medial heel with orthosis correlates to a decrease in pressure at plantar fascia (Image 10b) and the rearfoot motion occurring directly after initial impact characterizes use of frontal plane motion to mitigate shock at impact. **Reducing central heel pressure through force redistribution leads to a more stable, and balanced, loading pattern.**

Medial heel peak forces were additionally reduced bilaterally with orthosis ($p<0.001$) (Table 2). This statistically significant finding explains the benefits of improving rearfoot pronation (Image 10c). This circled pronation motion is the body's natural mechanism for dealing with shock that is generated by the repetitive collision seen in gait. **These study findings relate to an overall change in the foot's interaction with the ground and improved economy in walking gait with orthosis.**
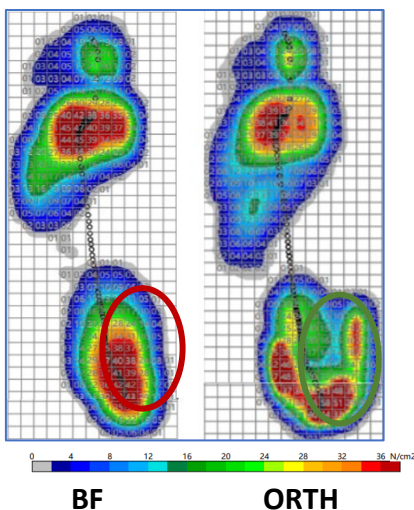
Image 10a. Reduced medial and central heel pressures.

Image10b: Plantar facia at medial heel. https://www.yehuwdah.com/foot-heel-ankle/heel-pain-plantar-fasciitis-achilles-tendon
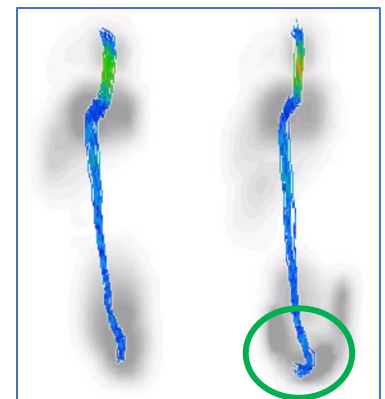
Image 10c: Pronation control at heel contact.

Additionally, supporting the significance of reduced medial and central heel pressures is the finding decreasing loading rates and reduced variability at heel contact. Below is the ground force reaction normative for barefoot

13

(yellow) and orthosis (blue) that visualizes this difference (Image 11a). The orthosis GFR displays a more linear rate of loading also supported by reduced variability (Image 11b). A smoother loading with reduced amounts of variability is represented in these curves (Image 11b, 12). With the orthosis, an almost 60% reduction in variability through loading was revealed (as evidenced by the circled area in Image 6b). **Reducing loading forces and reduced variability through loading results in improved shock absorption during heel strike as in a improved loading pattern.**
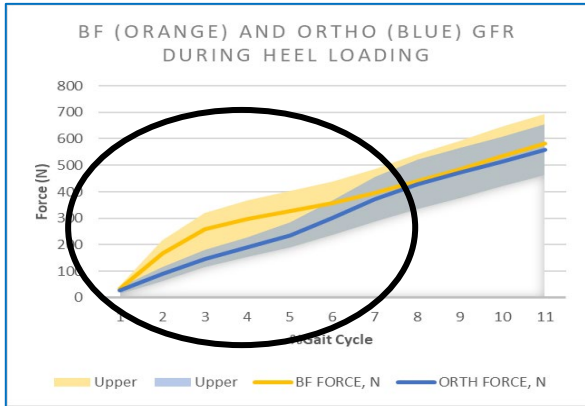
Image 11a: Zoomed in phase of loading.
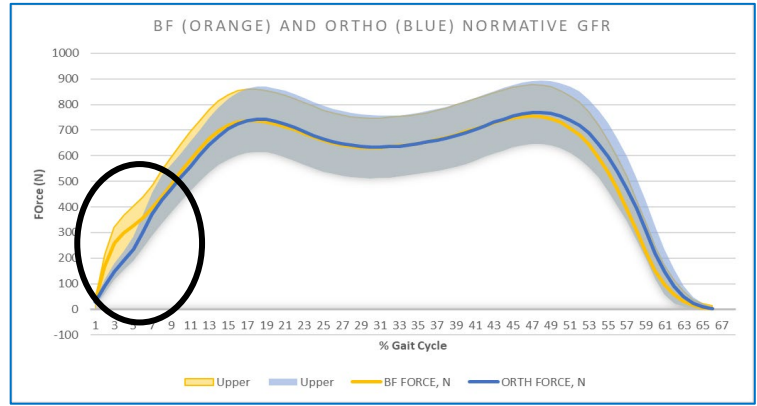
**11b:** Participant normative GFR with enhanced GFR characteristics through contact with device.
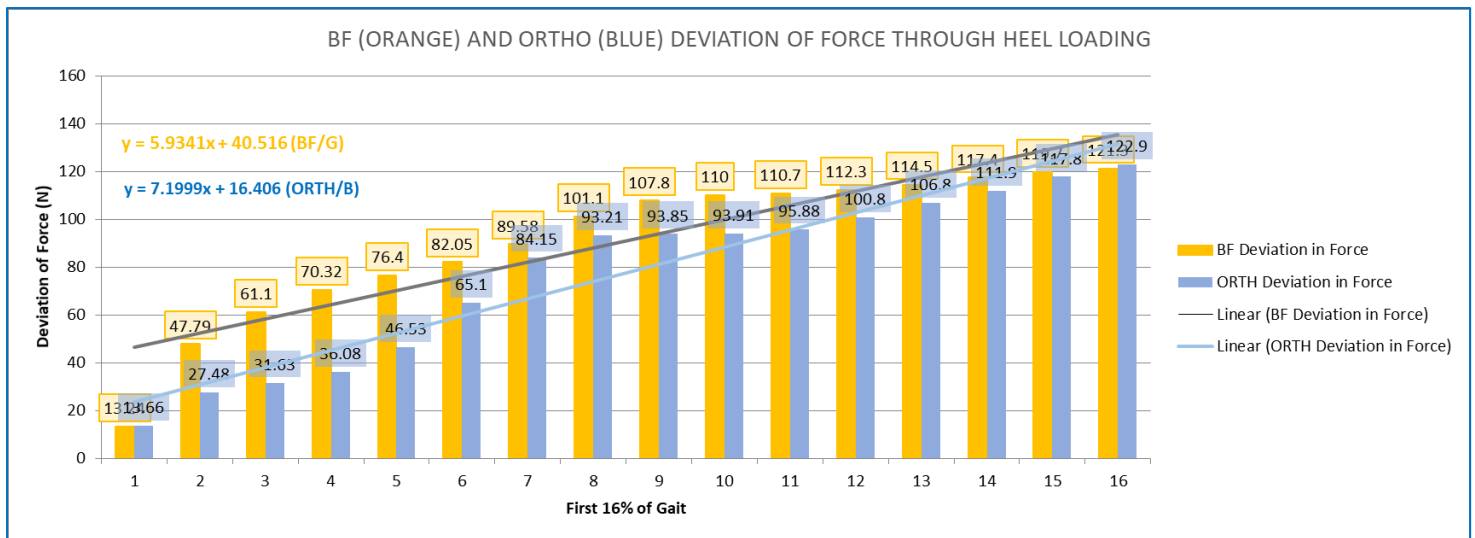
Image 12: Participant normative force curve of standard deviation of GFR through loading response with greatest deviation through contact.

Results with orthosis characterized more proximal and more medial exact locations of COP starting data with respect to the pressure at that instance (Image 13). As the COP progresses through loading response, a more neutral progression in the COP results with orthosis (Image 14). Metrics supporting this are found in the zonal pressure re-distributions, specifically through the lateral heel and the mid-foot (Table 2 and 3). Less medial COP progressions and ensuing reduced midfoot pressure distributions through midstance explains the more linear motion with optimized direction in orthosis (Image 9). **Results of straighter, more linear COP progression through loading response and mid-stance are consistent with improved foot efficiency and function based on clinical experience.**

BF **ORTH** **BF** **ORTH**
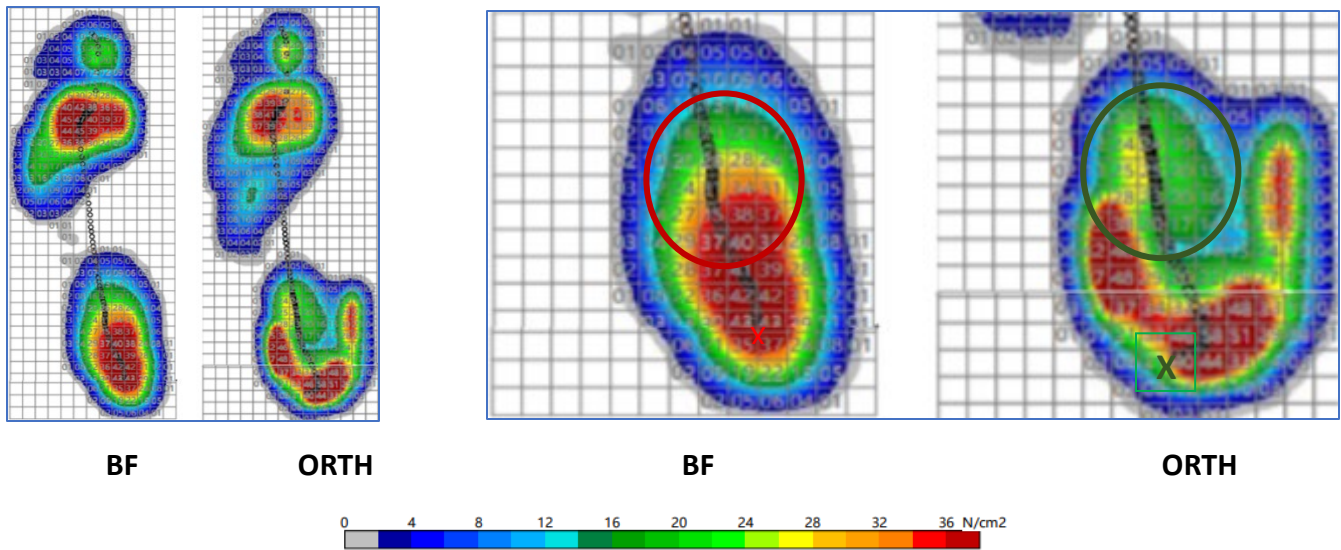
Image 13: 1:1 report visualizations displaying more distal IIP as well as excessive pronation control through loading.

BF **ORTH** **BF** **ORTH**
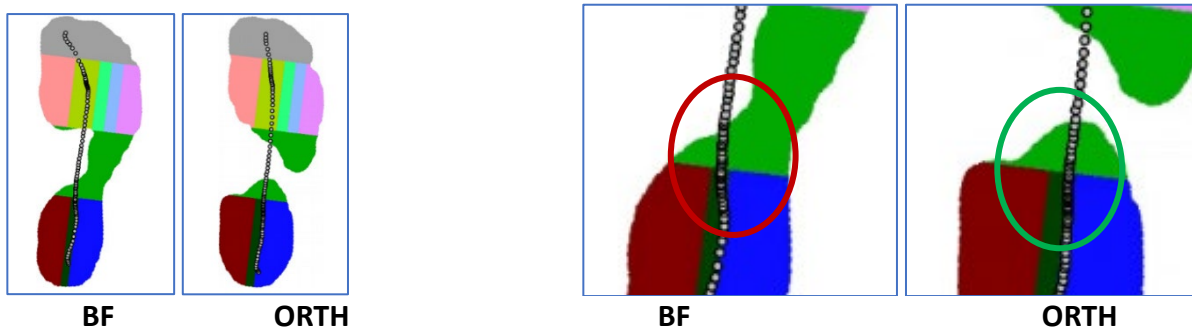
Image 14: Pronation control, and 27% less deviation in the mediolateral COP progression with orthosis.

As the COP progresses to the forefoot, additional reductions in pressure (N/mc2) results with orthosis. A 12.9% forefoot pressure reduction was measured with orthosis (Image 15a, b). In addition to the forefoot pressure reduction found with the orthosis was an improvement in the linearity of roll through in the forefoot (Image 16a, b). Peak pressure relief with orthosis resulted, along with redistribution and improvements in the morphology or direction of COP through gait propulsive phase. **This morphological improvement indicates a lasting effect of the orthosis shell after the distal portion is no longer in primary contact with the support surface.**
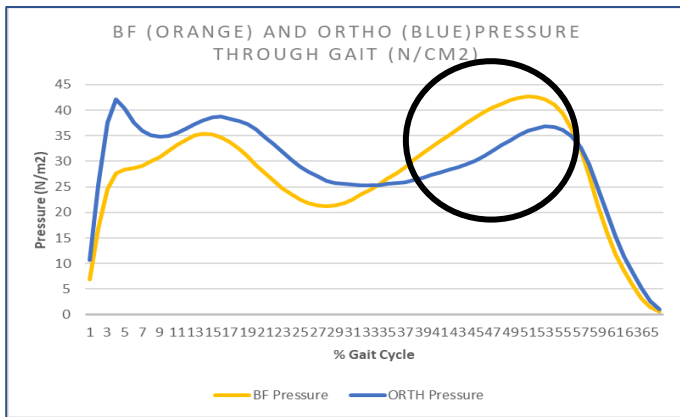
Image 15a: Pressure curve of population with 12.9% reduced pressure on metatarsals.
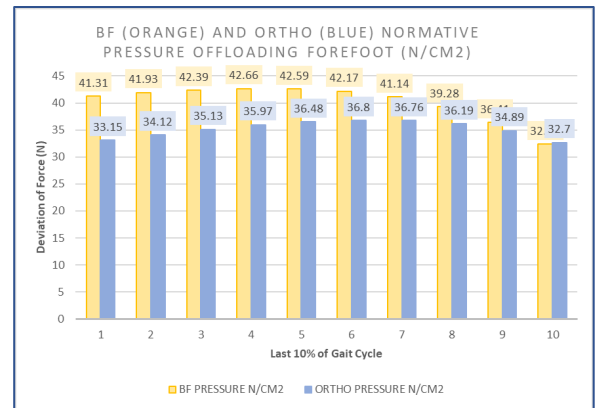
Image 15b: Zoomed in pressure difference at forefoot.
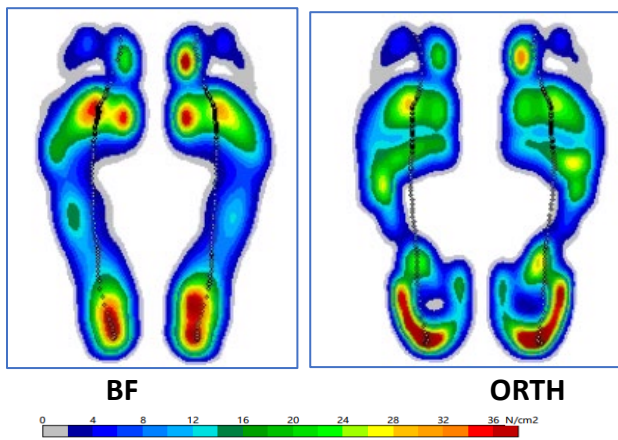
Image 16a: Reduced forefoot pressures under metatarsals and direction of progression through forefoot displaying improved efficiency.
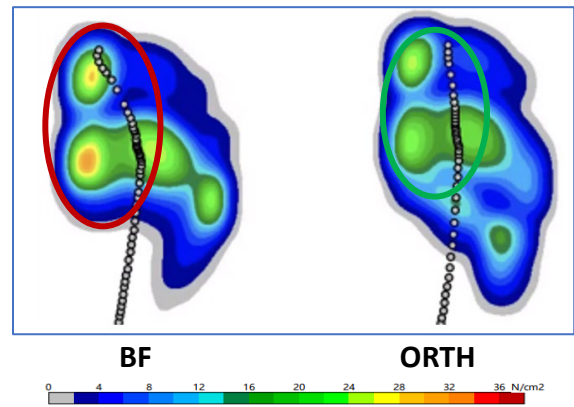
Image 16b: Visual of reduced pressure through forefoot.

One of the most comprehensive findings from the study was the overall decreased asymmetry with orthoses. Whether it was temporal (e.g. single support phase, variability in the single support phase, loading response of pre-swing phases) or spatial asymmetry is reduced (e.g. foot rotation, step length, length variability) or any of the variables from Table 2, the move to more symmetrical gait spatial and temporal measures is characterized. In fact, there was a 12.2% change between symmetry in barefoot walking to orthosis walking (Image 17). **This overall decreased asymmetry of parameters shows the notably significant impact of this orthosis.**

Table 4: Asymmetry in gait variables and difference

Asymmetry parameters	BF	ORTH	p value	Difference	Range
Asymmetry in single support variability	13.80%	11.40%	0.2580	-2.40%	0.01814 – 0.06643
Asymmetry in Single support	5.50%	4.20%	0.4590	-1.30%	0.021853 - 0.04788
Asymmetry in step length variability	11.90	10.70	0.5350	-1.20%	0.02779 – 0.05301
Asymmetry in foot rotation variability	10.70	10.00	0.7290	-0.70%	0.03393 – 0.04819
Asymmetry in Support phase	0.70%	0.07%	0.6310	-0.63%	0.00352 –0.00215
Asymmetry in loading response	3.70%	3.60%	0.9430	-0.10%	0.01698 – 0.01826
Asymmetry in Preswing phase	3.80%	3.70%	0.6620	-0.10%	0.01736 – 0.01790
Asymmetry in step length	2.10%	2.00%	0.9050	-0.10%	0.00993 – 0.011206

Negative values are not negative results, they represent decreasing asymmetry (moving towards optimal, 0%)
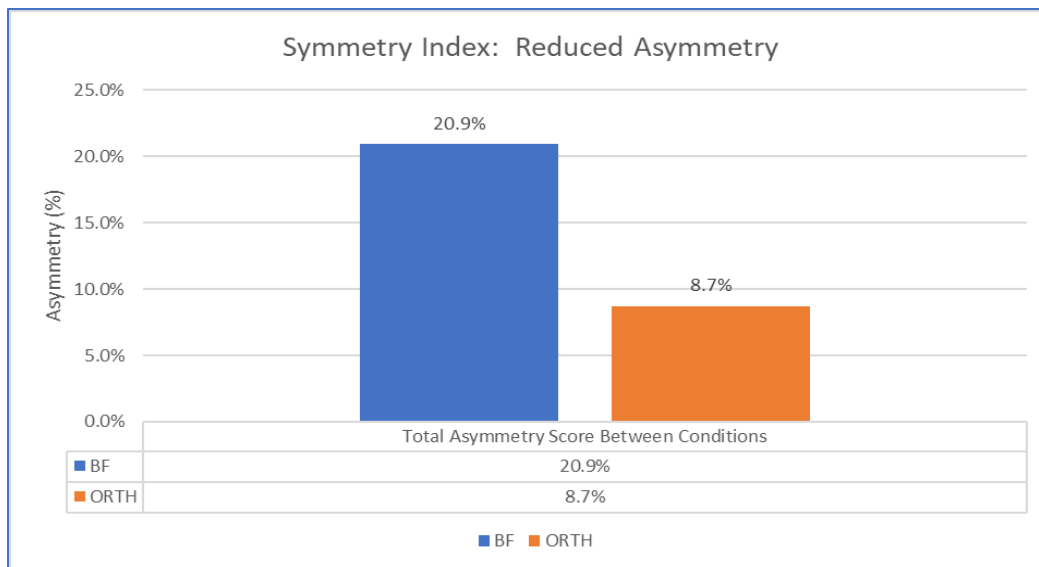
Image 17: Difference in total symmetry index changes between barefoot and orthosis walking.

Table 2. Comparison of Means of Gait Parameters and Mean Differences Between Orthosis and Baseline Barefoot Data in Dynamic Gait Analysis

| Variables	Without Orthosis	With Orthosis	P-value	Mean differences	Confidence intervals for the mean differences
Gait Line					
Length of gait line (left), mm	256.2 ± 2.0	273.9 ± 2.4	<0.001	-17.70826	-23.84317—-11.57335
Length of gait line (right), mm	253.9 ± 2.4	271.8 ± 2.6	<0.001	-17.92203	-24.82330—-11.02076
Spatial Pressure Parameters					
Anterior-posterior position, mm	143.8 ± 1.4	151.1 ± 1.3	<0.001	-7.34321	-11.20236 —-3.48405
Variability in anterior-posterior	3.4 ± 0.2	2.9 ± 0.1	0.016	0.46379	0.0867001—.8408853
Lateral symmetry, mm	2.2 ± 0.7	1.2 ± 0.5	0.248	1.05110	-0.74010 — 2.84230
Variability in lateral symmetry	2.9 ± 0.2	2.7 ± 0.1	0.434	0.17845	-0.27102 — 0.62793
Step width, cm	8.9 ± 0.4	8.0 ± 0.4	0.103	0.98020	-0.20004 — 2.1604
Variability in Step width	1.0 ± 0.3	0.9 ± 0.0	0.167	0.06953	-0.02948 0.16856
"Foot rotation" (left), in degrees	6.1 ± 0.4	7.3 ± 0.5	0.042	-1.28185	-2.51474-0.04895
"Foot rotation" (right), in degrees	7.9 ± 0.5	9.1 ± 0.5	0.113	-1.18559	-2.65457 — 0.28338
Variability in "foot rotation" (left), in degrees	6.1 ± 0.4	7.3 ± 0.5	0.0417	-1.28184	-2.514743— -0.04895
Variability in "foot rotation" (right), in degrees	1.4 ± 0.0	1.2 ± 0.0	0.0014	0.18949	0.07482 — 0.30417
Heel Pressure Parameters					
Ten zones Peak force RT HC	107.4 ± 2.4	81.3 ± 2.5	<0.001	26.10458	19.22619— 32.98296
Ten zones Start RT HL	0.04 ± 0.02	0.0 ± 0.0	0.0132	0.04347	0.009385 — 0.07757
Ten zones Peak force LT HC [N]	109.7 ± 2.0	80.2 ± 2.3	<0.001	29.53228	23.47091— 35.59365
Ten zones Start LT HL	0.07 ± 0.02	0.0 ± 0.0	0.006	0.06521	0.019558 0.110876

All data are reported as mean ± standard error

Table 3. Results of Multiple Linear Regression Analyses of Significant Gait Parameters Associated with 3D Printed Device in Dynamic (Negative is a decreasing variable)

Parameters	Regression Coefficient (95% CI)	P-value
Ten zones Start LT HL**	-0.065 (-0.113 - -0.017)	0.009
Variability in Foot rotation (internal/external foot position), SD**	-0.131 (-0.224 - -0.038)	0.006
Variability in anterior-posterior position*	-0.464 (-0.847 - -0.081)	0.018
Anterior-posterior position***	7.342 (3.442 – 11.244)	<0.001
Average length of gait line (left)	0.839 (-0.319 – 1.998)	0.154
Average length of gait line (right)	0.0130 (-1.008 – 1.115)	0.981

SD: Standard deviation; CI: Confidence interval, asterisk represents stronger power between barefoot and device

STANDING BALANCE RESULTS

During standing balance tasks, improved symmetry in average force through the rearfoot resulted. Forces in the rearfoot became more than 5.8% more balanced between limbs (p=0.037). Equal balance between limbs in standing explains a more stable balance is encouraged with orthosis. The below table depicts the multiple linear regression model of $Y = \beta + \beta_o x1 + \beta_1 x2 + \beta_2 x3 + \varepsilon$, where Y is the predictor or target variable and x1, x2, x3 are the independent variables. B is the y-intercept and β_o, β_1, β_2 and ε are the coefficients and error term respectively. Rather than simply using sample statistics to show that the majority of participants improved their symmetry in standing, these results help further explain the profound influence of orthosis in standing balance. **Even after adjusting for all cohort characteristics as well as interaction of all variables, significant effects of the orthosis condition on improving symmetry in distribution of forces between legs resulted**.

Table 4. Comparison of Means of Gait Parameters and Mean Differences Between Orthosis and Baseline Data in Static Gait Analysis

Variables	Without Orthosis	With Orthosis	P-value	Standardized mean difference	Confidence intervals for the mean difference
Standing Balance Force Parameters					
Forefoot Distribution	0.21953 ± 0.06	0.16347 ± 0.08	0.554	0.05607	-0.13271 — 0.24484
Rearfoot Distribution	0.78046 ± 0.06	0.83653 ± 0.08	0.554	-0.05607	-0.24485 — 0.13271
Center of Pressure Balance Parameters					
95% Confidence Ellipse Area	29.8 ± 8.4	17.7 ± 4.7	0.215	12.0625	-7.219844 — 31.34484
Length of minor axis, mm	3.7 ± 0.6	2.8 ± 0.3	0.155	0.93438	-.367957 — 2.23671
Length of major axis, mm	7.1 ± 1.0	6.2 ± 0.8	0.466	0 .91875	-1.58688 —3.42438
Deviation Right, mm	9.1 ± 1.14	8.2 ± 1.32	0.619	0.87188	-2.61165 — 4.35540
Deviation Forward, mm	-17.8 ± 2.2	-16.1 ± 2.4	0.587	-1.759375	-8.203781— 4.685031
Max. area left, cm²	90.8 ± 3.1	95.4 ± 3.0	0.251	-4.64375	-12.65966 — 3.372157
Max. area right, cm²	91.1 ± 3.7	93.2± 3.3	0.682	-2.04375	-11.96001 — 7.872509

All data are reported as mean ± standard error

Table 5. Multiple Linear Regression Analysis to Assess the Association of Rearfoot Asymmetry Gait Parameter with 3D Printed Orthosis Device in Standing Balance

Covariates	Regression Coefficient (95% CI)	P-value
Solution		
Baseline	Ref	
Orthosis	-0.05825 (0.00372 – 0.11277)	0.037
Gender		
Male	Ref	
Female	0.06705 (0.01327 – 0.12083)	0.015
Length of minor axis, mm	0.00793 (-0.00279 – 0.01866)	0.144
Rearfoot distribution	+0.09532 (-0.16864 - -0.02200)	0.012

CI: Confidence interval

DISCUSSION

The development of the efficacy protocol regimen in this honed, high-level study was designed to discover the effects of a 3D custom orthosis device with fixed additions and modifications on a human foot, both statically and dynamically. Given that shoes, varying shoe mechanics, and shoe interaction with individual kinematics add variability, testing directly on the human foot was completed. The isolation protocol choice resulted in clean data providing standardized comparison of a human foot before, and after 3D orthosis application, and how they relate to established norms.

Regarding the choice of the orthosis used in this efficacy study, additions and modifications must be discussed. It is common practice to further tailor a patient-specific orthosis shell with functional additions and modifications based on diagnosis and usage. These items were omitted from this study to ascertain the effects of this classic shell-centric prescription, which met the base needs of all participants. Inclusion of additions and modifications is planned for future work as such variability in the cohort would cloud the data. The pragmatic design and orthosis chosen allow a baseline to be established upon which further investigations may be completed.

Treadmill-based pressure instrumented systems may present limitations to whether a patient can naturally fit onto the pressure mapping surface in the treadmill. The ability to use a larger treadmill bed with appropriately configured four camera synchronization reduced this limitation in the discussed efficacy study. Having such a controlled environment for testing static and dynamic motions, with controlled velocities, with synchronized visual motion made the Noraxon CAGA suite the logical choice for this study.

CONCLUSION

The results of this focused efficacy study show the qualitative and quantitative effects of the functional Arize/HP 3D printed orthosis. They support conclusions of statistically significant positive trends/patterns in both spatial and temporal parameters in both standing and walking.

After adjusting for all population characteristics and interactions from all other variables, there was a very consolidated list of significant positive trends. As a summary of concluding statements, the influence of this orthosis on the barefoot for this cohort shows the following trends:

A lengthened or prolonged COP contact and stance phase with more forward motion in gait progression coinciding with reduced injury rates (Image 6 with Graph Images 7, 8), overall improvement in side-to-side shifting and variability in placement proving more optimal stability through gait with orthosis (Graph Images 9) (Table 2), reducing central heel pressure and direction of loading leading to a more stable, and balanced, loading pattern, changing in the foot's interaction with the ground representing improved pronation control with orthosis (Image 10), reduced loading forces and significantly reduced variability through loading results additionally supporting improved shock absorption during heel strike with orthosis (Image 11, 12), results of straighter, more linear COP progression through loading response and mid-stance consistent with improving foot efficiency and function based on clinical experience (Image 13), COP morphological improvements through the forefoot indicating a lasting effect of the orthosis shell after the distal portion is no longer in in primary contact with the support surface, overall reduced asymmetry of parameters while walking in orthosis (Table 4,

Image 17), and lastly in static balance significant reductions in asymmetry of force distributions between legs resulted (Table 4, 5).

Table 6. Results of Multiple Linear Regression Analyses of Significant Gait Parameters Associated with 3D Printed Device in Dynamic Walking

Parameters	Regression Coefficient (95% CI)	P-value
Ten zones Start LT HL	-0.065 (-0.113 - -0.017)	0.009
Variability in Foot rotation right, SD	-0.131 (-0.224 - -0.038)	0.006
Variability in anterior-posterior position	-0.464 (-0.847 - -0.081)	0.018
Anterior-posterior position	7.342 (3.442 – 11.244)	<0.001
Average length of gait line (left)	0.839 (-0.319 – 1.998)	0.154
Average length of gait line (right)	0.0130 (-1.008 – 1.115)	0.981
Ten zones peak force MF (left)	75.27 (44.08 – 106.45)	<0.001
Ten zones peak force MF (right)	52.15 (21.99 – 82.31)	0.001
Ten zones peak force HM (left)	0.89 (-1.93 – 3.71)	0.534
Ten zones Duration HL (left)	0.51 (-2.02 – 3.05)	0.688
Ten zones Duration HL (right)	1.43 (-0.92 – 1.20)	0.790
Left Foot Rotation (degrees)	1.282 (0.048 – 2.515)	0.042
Right Foot Rotation (degrees)	1.185 (-0.289 – 2.661)	0.114

SD: Standard deviation; CI: Confidence interval

DISCLOSURE

This study was commissioned by HP. None of the testing personnel are employees of HP, nor offer or dispense any HP products on a fee-for-service basis. All testing staff is familiar with and has worn the product being tested and has, in the past, given input to HP on future product, not to include the device being tested. All testing staff has done testing for other orthosis products and companies. One of the primary investigators holds patents related to foot care, but none of the said intellectual property has been licensed to HP/Arize or included in this study.

APPENDIX A

Complete Result Tables

Table 7. Comparison of Means of Gait Parameters and Mean Differences Between Orthosis and Baseline Data in Dynamic Gait Analysis

Variables	Without Orthosis	With Orthosis	P-value	Mean differences	Confidence intervals for the mean differences
Gait Line					
Average length of gait line (left), mm	256.2 ± 2.0	273.9 ± 2.4	<0.001	-17.70826	-23.84317 —-11.57335
Variability in average length of gait line (left), mm	4.7 ± 0.3	4.6 ± 0.4	0.804	0.12167	-0.84512 — 1.088554
Average length of gait line (right), mm	253.9 ± 2.4	271.8 ± 2.6	<0.001	-17.92203	-24.82330 —-11.02076
Variability in length of gait line (right), mm	5.1 ± 0.4	5.5 ± 0.5	0.527	-0.41481	-1.71115 — 0.88153
Single Support Line					
Average single support line (left), mm	133.5 ± 2.3	133.6 ± 2.8	0.975	-0.11272	-7.20415 — 6.97869
Variability in single support line (left), mm	6.0 ± 0.3	6.5 ± 0.4	0.337	-0.48641	-1.48413 — 0.51131
Average single support line (right), mm	126.6 ± 2.4	129.3 ± 2.7	0.464	-2.61643	-9.67187 — 4.43901
Variability in single support line (right), mm	6.6 ± 0.4	6.6 ± 0.4	0.969	0.02221	-1.10830 — 1.15270
Stance phase					
Stance phase (left), %	65.2 ± 0.3	65.6 ± 0.3	0.342	-0.37998	-1.16905 — 0.40909
Variability in Stance phase (left), SD	0.8 ± 0.0	0.8 ± 0.0	0.965	-0.00212	-0.09694 0.09270
Stance phase (right), %	65.0 ± 0.3	65.6± 0.3	0.175	-0.56616	-1.38790 — 0.25555
Variability in Stance phase (right), SD	0.81 ± 0.0	0.84 ±0.0	0.594	-0.02851	-0.13419 — 0.07716
Single Support					
Average single support, (left), mm	35.0 ± 0.3	34.4 ± 0.3	0.170	0.57714	-0.25016 — 1.40445
Variability in single support, (left), SD	0.9 ± 0.0	0.9 ± 0.0	0.915	-0.00541	-0.10525 — 0.09442
Average single support, (right), mm	34.8 ± 0.3	34.4 ± 0.3	0.340	0.38350	-0.40920 — 1.17623
Variability in single support, (right), SD	0.9 ± 0.0	0.9 ± 0.0	0.609	0.02289	-0.06554 — 0.11133
Phasic gait					
Load response, (left), mm	14.9 ± 0.3	15.3 ± 0.3	0.285	-0.45179	-1.28517 — 0.38158
Load response, (right), mm	15.4 ± 0.3	15.9 ± 0.3	0.203	-0.50261	-1.27957 — 0.27434
Variability in Load response, (left), SD	0.7 ± 0.0	0.7 ± 0.0	0.423	-0.02993	-0.1036339 --0.0437658
Variability in Load response, (right), SD	0.8 ± 0.0	0.8 ± 0.0	0.529	0.02340	-0.05002 — 0.09683
Preswing Phase (left)	14.9 ±0.3	15.3 ±0.3	0.282	-0.45759	-1.285169 — .2755879
Variability in Preswing Phase (left), SD	0.9 ± 0.0	0.8 ± 0.0	0.434	-0.00212	-0.09694 — 0.0926936
Preswing Phase (right)	15.4 ±0.3	15.9 ± 0.3	0.203	-0.50479	-1.29608 — .38089
Variability in Preswing Phase (Right), SD	0.8 ± 0.0	0.8 ± 0.0	0.257	-0.04502	-0.1233401 —0.033288
Swing phase (left), %	34.8 ± 0.2	34.4 ± 0.2	0.342	0.37998	-.409094 — 1.169053
Variability in Swing phase (left), SD	0.81 ± 0.0	0.82 ± 0.0	0.965	-0.00212	-0.09694 0.09269
Swing phase (right)	35.0 ± 0.3	34.4 ± 0.3	0.175	0.56617	-0.25555 — 1.38789
Variability in Swing phase (Right)	0.82 ± 0.0	0.84 ± 0.0	0.594	-0.02851	-0.13419 — 0.07716
Cadence Step	91.5 ± 1.7	92.8 ±1.8	0.593	-1.32579	-6.22072 — 3.56914
Variability in Cadence Step	1.7 ± 0.1	1.7 ± 0.1	0.800	-0.03771	-0.33299— 0.25756
Variability in Velocity Kmh	0.1 ± 0.0	0.1 ± 0.0	0.305	-0.00390	-0.01141 —.00361
Stride length (cm)	115.0 ±1.9	117.2± 2.1	0.436	-2.19760	-7.75778 — 3.36257
Variability in Stride length	2.1 ± 0.1	1.9 ± 0.1	0.234	0.19145	-0.12504 0.50793
Step time (left)	673.8 ±12.8	665.7 ±14.1	0.671	8.09672	-29.5836 — 45.77703
Step time (right)	669.9 ± 13.0	657.8 ± 13.3	0.512	12.06670	-24.82631 — 48.96028
Variability in Step time (right)	17.9 ± 1.2	17.3 ± 1.5	0.773	0.55829	-3.25638 4.37296
Stride time (ms)	1343.7 ± 25.7	1323.5 ± 27.3	0.592	20.16375	-54.03109 — 94.35858
Variability in stride time	26. 7 ± 2.0	26.5 ± 2.6	0.950	0.20305	-6.23245 — 6.638547
Spatial parameters					
Anterior-posterior position,	143.8 ± 1.4	151.1 ± 1.3	<0.001	-7.34321	-11.20236 —-3.48405
Variability in anterior-posterior position	3.4 ± 0.2	2.9 ± 0.1	0.016	0.46379	0.0867001 - 0.8408853
Lateral symmetry, mm	2.2 ± 0.7	1.2 ± 0.5	0.248	1.05110	-0.74010 — 2.84230

Variability in lateral symmetry	2.9 ± 0.2	2.7 ± 0.1	0.434	0.17845	-0.27102 — 0.62793
Step length (left)	57.8 ± 1.0	58.8 ± 1.1	0.568	-0.84379	-3.75938 — 2.07181
Variability in Step length (left)	1.4 ± 0.0	1.4 ± 0.0	0.720	0.03721	-0.16774 0.24218
Step length (right)	57.0 ± 1.0	58.4 ± 1.0	0.323	-1.37610	-4.12048 — 1.36828
Variability in Step length (right)	1.4 ± 0.1	1.3 ± 0.1	0.191	0.13039	-0.06585 0.32663
Step width, cm	8.9 ± 0.4	8.0 ± 0.4	0.103	0.98020	-0.20004 — 2.1604
Variability in Step width	1.0 ± 0.3	0.9 ± 0.0	0.167	0.06953	-0.02948 0.16856
Foot rotation (left), in degrees	6.1 ± 0.4	7.3 ± 0.5	0.042	-1.28185	-2.51474-0.04895
Foot rotation (right), in degrees	7.9 ± 0.5	9.1 ± 0.5	0.113	-1.18559	-2.65457 — 0.28338
Variability in foot rotation (left), in degrees	6.1 ± 0.4	7.3 ± 0.5	0.0417	-1.28184	-2.514743 — -0.04895
Variability in foot rotation (right), in degrees	1.4 ± 0.0	1.2 ± 0.0	0.0014	0.18949	0.07482 — 0.30417
Cadence step	91.5 ± 1.7	92.8 ±1.8	0.593	-1.32579	-6.22072 — 3.56914
Variability in Cadence Step	1.7 ± 0.1	1.7 ± 0.1	0.800	-0.03771	-0.33299— 0.25756
Variability in Velocity Kmh	0.1 ± 0.0	0.1 ± 0.0	0.305	-0.00390	-0.01141 —.00361
Heel Pressure Parameters					
Ten zones Peak force RT HC	107.4 ± 2.4	81.3 ± 2.5	<0.001	26.10458	19.22619 — 32.98296
Ten zones Start RT HL	0.04 ± 0.02	0.0 ± 0.0	0.0132	0.04347	0.009385 — 0.07757
Ten zones Duration LTHL	61.2 ± 1.0	63.2 ± 1.1	0.182	-1.97029	-4.87602 —0.93544
Ten zones Peak force LT HC [N]	109.7 ± 2.0	80.2 ± 2.3	<0.001	29.53228	23.47091— 35.59365
Ten zones Start LT HL	0.07 ± 0.02	0.0 ± 0.0	0.006	0.06521	0.019558 0.110876
Ten zones duration LT HL	61.2 ± 1.0	63.2 ± 1.1	0.182	-1.97029	-4.87602 —.93544
Asymmetry parameters					
Asymmetry in Gaitline	0.008 ± 0.00	0.01 ± 0.00	0.428	-0.00269	-0.00946 — 0.00407
Asymmetry in gaitline variability	0.174 ± 0.03	-0.261 ± 0.043	0.110	-0.08609	-0.19236 — 0.02016
Asymmetry in Single support	0.055 ± 0.01	0.042 ± 0.01	0.459	0.01301	-0.021853 — 0.04788
Asymmetry in single support variability	0.138 ± 0.02	-0.114± 0.01	0.258	0.02415	-0.01814 – 0.06643
Asymmetry in Support phase	0.007 ± 0.001	0.0007 ± 0.000	0.631	-0.00068	-0.00352 –0.00215
Asymmetry in support phase variability	0.114 ± 0.015	0.149 ± 0.017	0.134	-0.03466	-0.08035 –.01102
Asymmetry in loading response	-0.037± 0.005	0.036 ± 0.007	0.943	0.00063	-0.01698 – 0.01826
Asymmetry in loading response variability	0.107 ± 0.016	0.118 ± 0.013	0.608	-0.01063	-0.05185 – 0.03059
Asymmetry in single support phase	0.011 ± 0.002	0.013± 0.002	0.400	-0.00208	-0.00699 – 0.00282
Asymmetry in single support phase variability	0.09 ± 0.014	-0.10 ± 0.013	0.344	-0.01867	-0.05786 – 0.02050
Asymmetry in Preswing phase	0.038 ± 0.006	0.037 ± 0.007	0.662	0.00027	-0.01736 – 0.01790
Asymmetry in preswing phase variability	0.097 ± 0.016	0.12 ± 0.015	0.303	-0.02354	-0.06882 – 0.021733
Asymmetry in swing phase	0.011 ± 0.002	0.013 ± 0.002	0.574	-0.00140	-0.00632 – 0.00354
Asymmetry in swing phase variability	0.1114 ± 0.015	-0.149 ± 0.017	0.134	-0.03466	-0.08035 – 0.01102
Asymmetry in Foot rotation	2.52 ± 2.29	0.18 ± 0.03	0.312	2.34669	-2.30753 – 7.00091
Asymmetry in foot rotation variability	0.107 ± 0.015	0.100 ± 0.014	0.729	0.00713	-0.03393 – 0.04819
Asymmetry in step length	0.021 ± 0.004	0.020 ± 0.003	0.905	0.00561	-0.00993 – 0.011206
Asymmetry in step length variability	-0.119 ± 0.012	0.107 ± 0.016	0.535	-.0338828	-0.02779 – 0.05301

All data are reported as mean ± standard error

Table 8. Comparison of Means of Gait Parameters and Mean Differences Between Orthosis and Baseline Data in Static Gait Analysis

Variables	Without Orthosis	With Orthosis	P-value	Standardized mean difference	Confidence intervals for the mean difference
Standing Balance Force Parameters					
Forefoot asymmetry	-0.00268 ± 0.01	-0.00166 ± 0.02	0.969	-0.0010	-0.0542746 — .0522487
Rearfoot asymmetry	-0.00875 ± 0.02	0.03674 ± 0.02	0.130	-0.04549	-0.10472 — 0.0137396
Forefoot Distribution	0.21953 ± 0.06	0.16347 ± 0.08	0.554	0.05607	-0.13271 — 0.24484
Rearfoot Distribution	0.78046 ± 0.06	0.83653 ± 0.08	0.554	-0.05607	-0.24485 — 0.13271
Maximum Back Force (Left)	238.4 ± 11.2	237.5 ± 10.3	0.955	0.86079	-29.50749 — 31.22906
Maximum Back Force (Right)	243.1 ±12.3	222.9±12.1	0.247	20.15503	-14.28093 — 54.59099
Maximum Front Force (Left)	173.2 ± 9.0	182.0 ± 8.7	0.486	-8.78638	-33.84716 — 16.27441
Maximum Front Force (Right)	172.9± 7.9	184.0 ± 9.8	0.384	-11.08919	-36.37373 — 14.19536
Center of Pressure Balance Parameters					
95% Confidence Ellipse Area	29.8 ± 8.4	17.7 ± 4.7	0.215	12.0625	-7.219844 — 31.34484
COP Pathlength, mm	22.3 ± 4.5	22.4 ± 5.3	0.989	-0.09375	-13.99242 — 13.80492
COP average velocity, mm/sec	1.9 ± 0.4	1.8 ± 0.4	0.822	0.12500	-0.98237 — 1.23237
Length of minor axis, mm	3.7 ± 0.6	2.8 ± 0.3	0.155	0.93438	-.367957 — 2.23671
Length of major axis, mm	7.1 ± 1.0	6.2 ± 0.8	0.466	0 .91875	-1.58688 — 3.42438
Angle between forward and major axis, deg	42.3 ± 4.9	53.6 ± 5.1	0.114	-11.25625	-25.29066 — 2.77816
Deviation Right, mm	9.1 ± 1.14	8.2 ± 1.32	0.619	0.87188	-2.61165 — 4.35540
Deviation Forward, mm	-17.8 ± 2.2	-16.1 ± 2.4	0.587	-1.759375	-8.203781 — 4.685031
Max. area left, cm²	90.8 ± 3.1	95.4 ± 3.0	0.251	-4.64375	-12.65966 — 3.372157
Max. area right, cm²	91.1 ± 3.7	93.2± 3.3	0.682	-2.04375	-11.96001 — 7.872509

All data are reported as mean ± standard error

Table 9. Multiple Linear Regression Analysis to Assess the Association of Rearfoot Asymmetry Gait Parameter with 3D Printed Orthosis Device in Standing Balance

Covariates	Regression Coefficient (95% CI)	P-value
Solution		
Baseline	Ref	
Orthosis	-0.05825 (0.00372 – 0.11277)	0.037
Gender		
Male	Ref	
Female	0.06705 (0.01327 – 0.12083)	0.015
Length of minor axis, mm	0.00793 (-0.00279 – 0.01866)	0.144
Rearfoot distribution	+0.09532 (-0.16864 - -0.02200)	0.012

CI: Confidence interval

The above table depicts the multiple linear regression model of $Y = \beta + \beta_o x1 + \beta_1 x2 + \beta_2 x3 + \varepsilon$
where Y is the predictor or target variable and x1, x2, x3 are the independent variables. β is the y-intercept and β_o, β_1, β_2 and ε are the coefficients and error term respectively.

Table 10. Results of Multiple Linear Regression Analyses of Significant Gait Parameters Associated with 3D Printed Device in Dynamic

| Parameters	Regression Coefficient (95% CI)	P-value
Ten zones Start LT HL	-0.065 (-0.113 - -0.017)	0.009
Variability in Foot rotation right, SD	-0.131 (-0.224 - -0.038)	0.006
Variability in anterior-posterior position	-0.464 (-0.847 - -0.081)	0.018
Anterior-posterior position	7.342 (3.442 – 11.244)	<0.001
Average length of gait line (left)	0.839 (-0.319 – 1.998)	0.154
Average length of gait line (right)	0.0130 (-1.008 – 1.115)	0.981

SD: Standard deviation; CI: Confidence interval

Table 11. Multiple Linear Regression Analysis to Assess the Association of Variability in Foot rotation (right) Parameter with Orthosis in Dynamic

Covariates	Regression Coefficient (95% CI)	P-value
Solution		
Baseline	Ref	
Orthosis	-0.131 (-0.224 - -0.038)	0.006
Step length (right)	0.176 (0.091 – 0.261)	<0.001
Variability in step width	0.427 (0.25 – 0.598)	<0.001
Variability in foot rotation (left)	0.143 (0.0189 – 0.268)	0.024

CI: Confidence interval

APPENDIX B

COP GAIT CYCLE
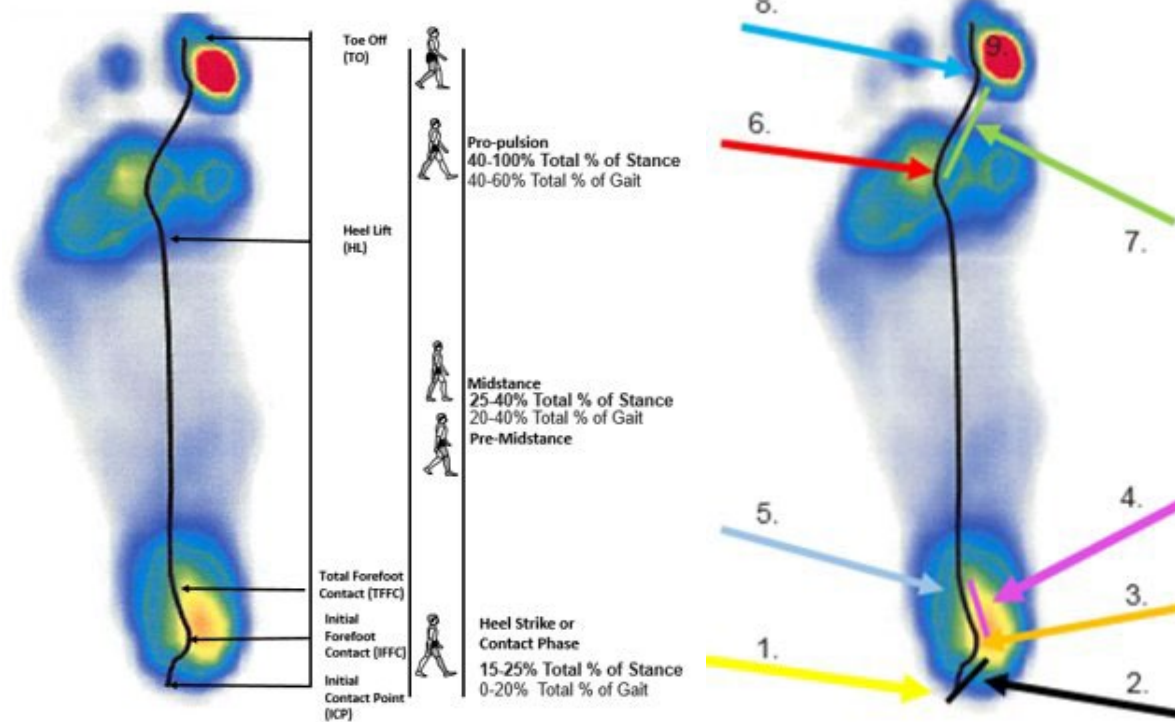
COP GAIT CYCLE EVENTS

1. Initial Contact Point (often the first intersection with neutral)
2. Initial Contact Response
3. End Initial Contact Response Point
4. Initial Single Support Curve (during contact phase or loading response)
5. Re-supination Point (often the second intersection with neutral)
6. Terminal Transition Point (often the third intersection with neutral)
7. Forefoot Pronation Curve
8. Terminal Double Support
9. Toe-Off Curve
10. Toe-Off Point

INTEGRATED SOFTWARE SAMPLE SCREEN SHOTS

**Comprehensive snapshot of the data collection during Dynamic Gait Testing**
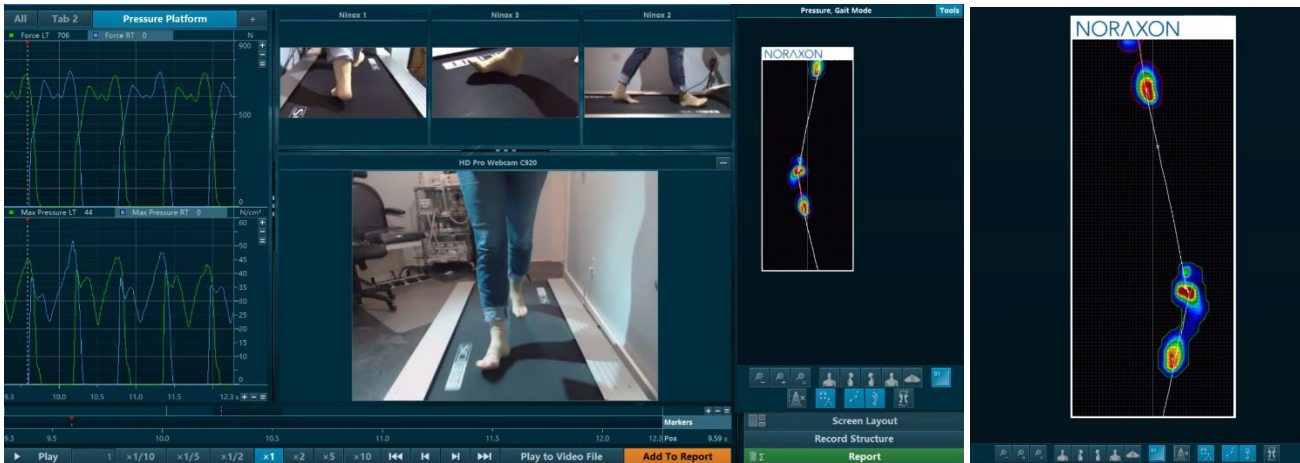
SAMPLE REPORTING VIEW
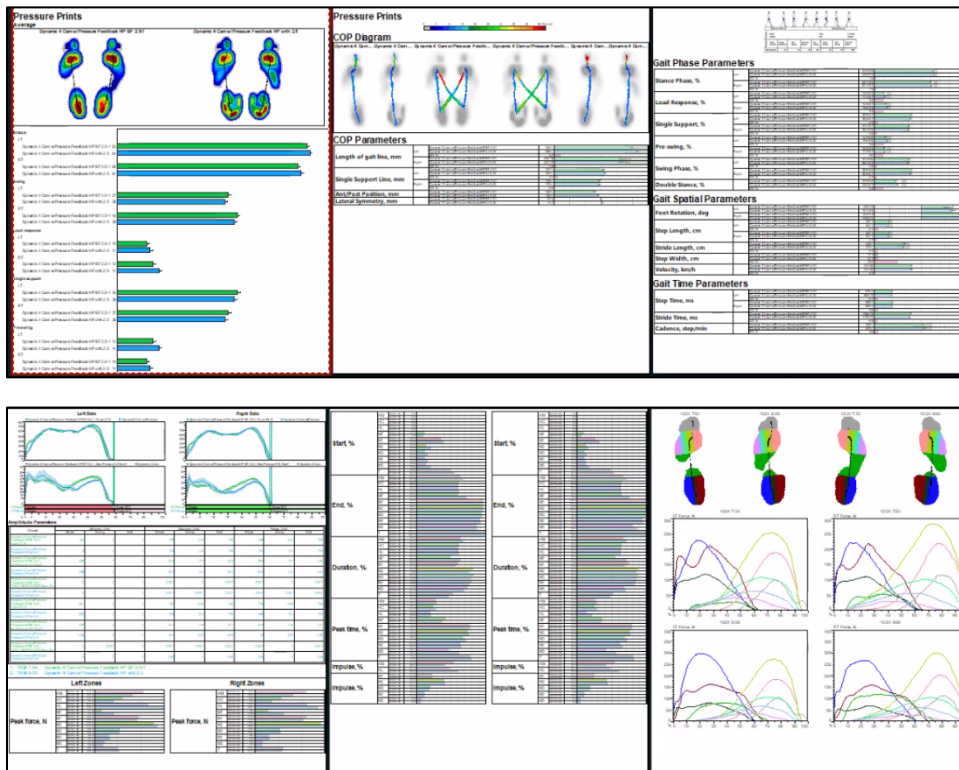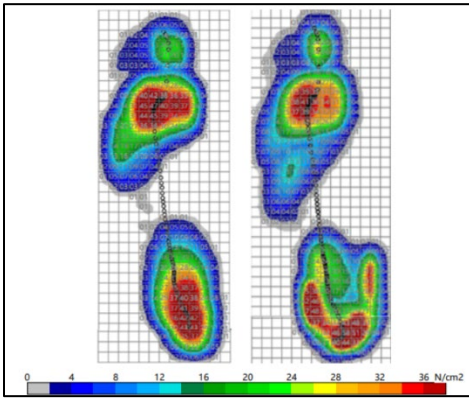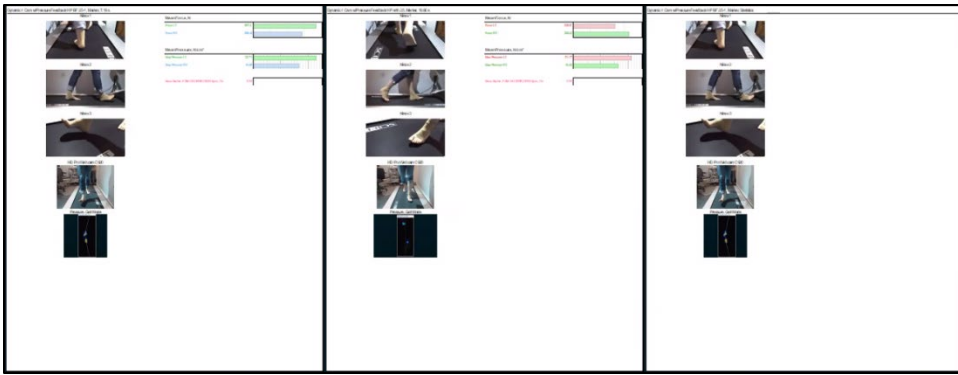
APPENDIX C

Consent

PROTOCOL AND CONSENT TO PARTICIPATE
We would like to invite you to participate in a study designed to understand more about the impact of 3d printed orthosis on movement gait kinetics and balance when compared to barefoot movement gait kinetics and balance.
Although there is no direct benefit to you if you choose to participate, this study will significantly contribute to our current understanding of precision custom orthosis impacts on biomechanics.
 PROTOCOL FOR PARTICIPANTS;
1. Visit 1: Scheduled Scan and Eval Completed with consented participant -
    a. 3d Scan Process and Imaging
    b. Patient Evaluation including 2.8mph barefoot dynamic barefoot with Custom sock (40-120sec on treadmill, hands resting on front console support, last 30 seconds of walking being recorded), all metrics analyzed via CUSTOM REPORTS
    c. Optional static scan barefoot with Custom sock
        i. Static barefoot pressure scan with Custom sock (20-30seconds standing), all metrics analyzed via CUSTOM REPORT
2. In between visits provider will
a. Write Orthosis prescription
b. Receive Orthosis
c. Check orthosis against order and evaluation
3. Visit 2: Scheduled office visit
a. Take CAGA* repeat scan if needed- dynamic barefoot with Custom sock 2.8mph (40-120sec on treadmill, hands resting on front console support, last 30 seconds of walking being recorded), all metrics analyzed via CUSTOM REPORTS
    i. Static barefoot pressure scan with Custom sock (20-30seconds standing), all metrics analyzed via CUSTOM REPORT
b. Receive dispensed Orthosis, strap to foot with FS5 Or version with less compression
c. Take CAGA* scan – 2.8mph dynamic walking with custom sock with custom printed orthosis (sulcus length) (40-120sec on treadmill, hands resting on front console support, last 30 seconds of walking being recorded), all metrics analyzed via CUSTOM REPORTS
d. Optional static scan barefoot with Custom sock and 3D printed orthosis
    i. Static barefoot pressure scan with Custom sock and 3D printed sulcus length orthosis (20-30seconds standing), all metrics analyzed via CUSTOM REPORT

Overview:
Data Collection Equipment used in your testing:
* Instrumented Treadmill and Video Motion Analysis
* Noraxon software for hardware synchronization and analysis
A comprehensive clinical gait analysis test includes physical examination, videotaping, computerized gait analysis systems, recording of ground reaction forces between the feet and surface. Motions and forces are measured to assess the patient's status and to develop an appropriate treatment plan. Each component of gait analysis testing can be performed separately, but the data are most useful when viewed together in a comprehensive evaluation.

Voluntary Participation
Participating in this study is completely voluntary. Even if you initially decide to participate, you may change your mind and stop participation at any time. You may choose not to complete any survey or test, and you may withdraw from the study at any time, including before, during, or after any tasks, for any reason and without explanation.

Benefits
If you agree to take part in this study, there will be no direct benefit to you. This study is not designed to treat any illness or provide any positive health benefits for those who participate. You will not be compensated for your participation in this study.

Confidentiality of Information

NOTE: One risk of participating in any research is a loss of privacy. There is no legal privilege between investigator and subjects as there is between physician and patient or counselor and client. Thus, we do not give or imply a guarantee of "complete" or "strictest" confidentiality.

Data Sharing

Results of this research will be used for the purposes described in this study. This information may be published or shared at meetings, but you will not be identified. To keep your information safe, data will be identified by code number only, and will be kept separate from any information that could identify you. This is done to protect your privacy and to ensure that your health information is kept confidential.

De-identified data from this study may be shared with the research community at large to advance science and health. We will remove or code any personal information (e.g., your name, date of birth) that could identify you before files are shared with other researchers to ensure that, by current scientific standards and known methods, no one will be able to identify you from the information or samples we share. Despite these measures, we cannot guarantee anonymity of your personal data.

Due to the nature of this study, your individual results from cognitive testing, blood draws, and other measures will not be shared with you. This is to help protect your privacy and sensitive health information, and make sure that your data remains confidential.

Use of your information for future research

All identifiable information (e.g., your name, address, date of birth) will be removed from the information or samples collected in this project. After we remove all identifiers, the information or samples may be used for future research or shared with other researchers without your additional informed consent.

Questions

If you have any questions about this project or your participation, please feel free to ask questions now or contact Sally Crawford scrawford@myresiliencecode.com, 303-577-1935 at any time.

You may print or save a copy of this consent form if you would like one for your records. Please feel free to ask any questions about this study or consent either now or in the future by contacting Dr. Segel.

Signing the consent form

By clicking the link below, I confirm that I have read this form and decided that I will participate in the project described above. Its general purposes, the particulars of involvement have been explained to my satisfaction. I understand that I can discontinue participation at any time.

Please place an X next to the statement that indicates your choice for the options below:

_____ I voluntarily agree to participate in this study.

_____ I decline to participate in this study.

_____ The researchers may NOT contact me again to participate in future research activities.

_____ The researchers may contact me again to participate in future research activities.

Last, First: Signature: Date:

REFERENCES

1. Błażkiewicz M, Wiszomirska I, Wit A. Comparison of four methods of calculating the symmetry of spatial-temporal parameters of gait. Acta Bioeng Biomech. 2014;16(1):29-35. PMID: 24708092.
2. Hausdorff, J.M. Gait variability: methods, modeling and meaning. *J NeuroEngineering Rehabil* 2, 19 (2005). https://doi.org/10.1186/1743-0003-2-19
3. Heiderscheit, B. C., Hamill, J., & van Emmerik, R. E. (2002). Variability of Stride Characteristics and Joint Coordination among Individuals with Unilateral Patellofemoral Pain, Journal of Applied Biomechanics, 18(2), 110-121. Retrieved Oct 31, 2021, from https://journals.humankinetics.com/view/journals/jab/18/2/article-p110.xml).
4. Kalron A. Association between perceived fatigue and gait parameters measured by an instrumented treadmill in people with multiple sclerosis: a cross-sectional study. J Neuroeng Rehabil. 2015;12:34. doi:10.1186/s12984-015-0028-2.
5. Laroche DP, Cook SB, Mackala K. Strength asymmetry increases gait asymmetry and variability in older women. *Med Sci Sports Exerc*. 2012;44(11):2172-2181. doi:10.1249/MSS.0b013e31825e1d31
6. Alves SA, Ehrig RM, Raffalt PC, Bender A, Duda GN, Agres AN. Quantifying Asymmetry in Gait: The Weighted Universal Symmetry Index to Evaluate 3D Ground Reaction Forces. *Front Bioeng Biotechnol*. 2020;8:579511. Published 2020 Oct 23. doi:10.3389/fbioe.2020.579511
7. Nasirzade A, Sadeghi H, Mokhtarinia H R, Rahimi A. A Review of Selected Factors Affecting Gait Symmetry. PTJ. 2017; 7 (1) :3-12 URL: http://ptj.uswr.ac.ir/article-1-256-en.html
8. Hoffman JR, Ratamess NA, Klatt M, Faigenbaum AD, and Kang J. Do bilateral power deficits influence direction-specific movement patterns? Res Sports Med 15: 1–8, 2007.
9. Bell DR, Sanfilippo JL, Binkley N, and Heiderscheit BC. Lean mass asymmetry influences force and power asymmetry during jumping in collegiate athletes. J Strength Cond Res 28: 884–891, 2014.
10. Santos PCRd, Barbieri FA, Zijdewind I, Gobbi LTB, Lamoth C, Hortobaǵyi T (2019) Effects of experimentally induced fatigue on healthy older adults' gait: A systematic review. PLoS ONE 14 (12): e0226939. https://doi.org/10.1371/journal. pone.0226939.
11. Read P.J., Oliver J.L., Croix M.B.D.S., Myer G.D., Lloyd R.S. Neuromuscular risk factors for knee and ankle ligament injuries in male youth soccer players. Sports Med. 2016;46:1059–1066. doi: 10.1007/s40279-016-0479-z.
12. MARSK A. Studies on weight-distribution upon the lower extremities in individuals working in a standing position: assessing the results of the measurements of load-pressure differences against the background of handedness and some clinical observations. Acta Orthop Scand Suppl. 1958;31:1-64. doi: 10.3109/ort.1958.29.suppl-31.01. PMID: 13594397.
13. Kiesel KB, Butler RJ, Plisky PJ. Prediction of injury by limited and asymmetrical fundamental movement patterns in american football players. J Sport Rehabil. 2014 May;23(2):88-94. doi: 10.1123/jsr.2012-0130. Epub 2013 Nov 14. PMID: 24225032.
14. Segel, J, Crawford, S. Oct 2015. NYCPM, Wound Care Seminar: Computer Aided Gait Analysis for Orthotic Management.
15. Barry Meadows, Roy Bowers, Elaine Owen, 18 - Biomechanics of the Hip, Knee, and Ankle, Editor(s): Joseph B. Webster, Douglas P. Murphy, Atlas of Orthoses and Assistive Devices (Fifth Edition), Elsevier, 2019, Pages 207-215.e1, ISBN 9780323483230, https://doi.org/10.1016/B978-0-323-48323-0.00018-4. (https://www.sciencedirect.com/science/article/pii/B9780323483230000184
16. [i] Blair SJ, Lake MJ, Sterzing T, Cheung JT-M (2013). Lower extremity biomechanics following a period of adaptation to wearing unstable shoes, Footwear Science, 5(Suppl 1), S139-S141, 11. Footwear Biomechanics Symposium, Natal, Brazil.
17. Faude O, Donath L, Roth R, Fricker L, Zahner L. Reliability of gait parameters during treadmill walking in community-dwelling healthy seniors. Gait Posture. 2012 Jul;36(3):444-8. doi: 10.1016/j.gaitpost.2012.04.003. Epub 2012 May 1. PMID: 22555061.
18. Shorter K, Polk J, Rosengren K, Hsaio-Wecksler E. A new approach to detecting asymmetries in gait. Clin Biomech 23: 459–467, 2008.
19. Exell, T. A., Irwin, G., Gittoes, M. J. R., & Kerwin, D. G. (2012). Implications of intra-limb variability on asymmetry analyses. Journal of Sports Sciences, 30(4), 403-409. https://doi.org/10.1080/02640414.2011.647047.
20. Twisk J, Proper K. Evaluation of the results of a randomized controlled trial: how to define changes between baseline and follow-up. J Clin Epidemiol. 2004 Mar;57(3):223-8. doi: 10.1016/j.jclinepi.2003.07.009. PMID: 15066681.